

Topological reponse theory for flow networks

Henrik Ronellenfitsch,¹ Debsankha Manik,¹ and Dirk Witthaut^{2,3}

¹Max Planck Institute for Dynamics and Self-Organization (MPIDS), 37077 Göttingen, Germany

²Forschungszentrum Jülich, Institute for Energy and Climate Research - Systems Analysis and Technology Evaluation (IEK-STE), 52428 Jülich, Germany

³Institute for Theoretical Physics, University of Cologne, 50937 Köln, Germany

(Dated: April 14, 2015)

We analyze the response of a flow network to local damages or link failures. Using a dual representation in terms of cycle flows, we can predict the change of networks flows in an intuitive way using only on the topology of the network. As an example we show that the effect of transmission line failures in power grids can be understood from purely topological features of the network.

I. INTRODUCTION

Transportation, or flow networks are a key concept in the modeling of many natural as well as man made complex systems. Important examples include power grids (flow of energy), river basins (flow of water on a grand scale), or the vascular network of mammals and plants (flow of blood and water, respectively). In order to maintain their functionality, many such systems need to be designed to be robust against damage. This task can be taken over either by humans (power grids) or evolution through natural selection (vascular networks). However, because of the complex nature of many flow networks, predicting the effects of a perturbation can be challenging, as they depend strongly on the precise details such as position of the damaged edge. Therefore, investigating the effects of perturbations in complex flow networks is an important endeavour, not only to improve the design of man made systems, but also to further our understanding of evolutionary processes.

In this work we study the linearized effect of perturbations in planar networks which can be used to describe e.g. the venation network in vascular plant leaves, which is naturally planar, or power grids, which can be taken to be planar to a good approximation. We take a point of view dual to previous work, expressing the effect of a small perturbation in terms of cycle currents on the fundamental cycles (facets) of the networks. We show that a small perturbation induces two domains of oppositely oriented cycle currents on the network whose strength decays with shortest path distance on the dual graph and provide an algorithm that uses network topology to predict the direction of flow change due to the perturbation. We then proceed to apply our theory to two important test cases. First, we consider the linear flow network in one leaf of Norway maple (*Acer platanoides*) which was chemically cleared, scanned and had its network vectorized. We show that in this case, decay of the cycle currents is exponential. Second, we apply our method to the prediction of blackouts in nonlinear power grids, comparing the topologically predicted direction of flow change with numerically exact simulations, finding perfect agreement.

II. THE CONTINUITY EQUATION AND ITS DUAL REPRESENTATION

The *continuity equation* is the fundamental relation describing the steady state of a flow network: The sum of all flows to or from a node j must equal the source or sink strength P_j :

$$\sum_{\ell=1}^N F_{j\ell} = P_j. \quad (1)$$

In many important applications the flow is proportional to the potential drop along the edge. More general, we consider networks, where the flow is given by

$$F_{j\ell} = K_{j\ell} f(\phi_\ell - \phi_j) \quad (2)$$

with an antisymmetric function $f(\cdot)$ and the transport capacity or conductivity $K_{j\ell} = K_{\ell j}$. The steady state of the network is then determined by the equations

$$\sum_{\ell=1}^N K_{j\ell} f(\phi_\ell - \phi_j) = P_j. \quad (3)$$

for all $j = 1, \dots, N$ nodes of the network. This holds for DC electric circuits ('Kirchhoffs' law'), hydraulic networks [1] or vascular networks of plants [2]. AC power grids, which form the basis of our technical infrastructure, are discussed in more detail in section VI. Equation (3) also describes the steady state of oscillator networks such as the celebrated Kuramoto model [3–5], where ϕ_j is a phase variable.

An important question in network operation is the resilience to local damages: How does the network respond when the capacity of a single edge $K_{j\ell}$ is reduced or vanishes entirely? Is it stable or does the local failure induce a global blackout? Here we introduce a geometric theory of flow re-distribution after local damages based on the *dual representation* of the network flow problem. To this end we introduce the edge incidence matrix $E \in \mathbb{R}^{N \times L}$, L being the total number of edges [6]. The elements of the matrix are $E_{j,e} = 1$ if the node j is the head of the edge e , $E_{j,e} = -1$ if j is the tail of e and $E_{j,e} = 0$ otherwise. For the calculations we have to choose an orientation of

the edges, which is arbitrary but must be kept fixed. The continuity equation (1) then reads

$$\sum_{e=1}^L E_{j,e} F_e = P_j \quad (4)$$

This is an underdetermined equation for the flows, whose solutions span an $(L-N+1)$ -dimensional affine subspace. The homogeneous solutions correspond to *cycle flows* in the network, which do not affect the flow balance at the nodes.

Lemma 1. *All solutions to the continuity equation can be expressed as*

$$F_e = F_e^{(0)} + \sum_{c=1}^{L-N+1} f_c C_{c,e}, \quad f_c \in \mathbb{R}, \quad (5)$$

where $F_e^{(0)}$ is one special solution of the inhomogeneous equation.

If the flows are given by equation (2), we must further assume that the potentials or phases ϕ_j are unique. This condition is satisfied if the potential differences $\phi_j - \phi_i$ summed around each basis cycle of the network add up to zero (modulo 2π if ϕ_j is a phase variable). If the function f is invertible, this condition can be written in terms of the flows as

$$\sum_{e=1}^L C_{c,e} f^{-1}(F_e/K_e) = 0. \quad (6)$$

The coupling function f must be strictly monotonic to be invertible. For the sake of definiteness we assume that f is strictly monotonically increasing w.l.o.g. This is automatically satisfied for a potential flow where f is just the identity. If we are dealing with phase variables and a sinusoidal coupling function, we must demand that all phase differences are in the interval $(-\pi/2, +\pi/2)$. Notably, this guarantees the dynamic stability of an oscillator network [7].

Now we consider the case that the capacity of a single edge e_0 is slightly perturbed, $K'_{e_0} = K_{e_0} + \kappa$. To restore the phase condition (6) without affecting the continuity equation (4), we must add a suitable amount of cycle flows to the network. To calculate the perturbed solution explicitly, we choose the flows in the unperturbed network as the special solution $F_e^{(0)}$ in the decomposition (5). Expanding equation (6) to leading order in κ then yields a linear set of equations for the induced cycle flows

$$\sum_{c=1}^{L-N+1} A_{d,c} f_c = \kappa q_d. \quad (7)$$

The matrix A is given by

$$A_{d,c} = \sum_{e=1}^L C_{d,e} C_{c,e} g(F_e^{(0)}/K_e), \quad (8)$$

where g denotes the derivative of the inverse of the coupling function, $g = (f^{-1})'$. The inhomogeneity

$$q_d = C_{d,e_0} g(F_{e_0}^{(0)}/K_{e_0}) F_{e_0}^{(0)}/K_{e_0} \quad (9)$$

is non-zero only for the two cycles adjacent to edge e_0 . Calling these two cycles c_1 and c_2 , we have $q_{c_1} = -q_{c_2}$. If the edge e_0 lies on the boundary of the network, only one element is non-zero.

III. TOPOLOGY OF CYCLE FLOWS

Equation (7) determines the linear response of the network to local perturbations. The formulation directly yields the flows F_e instead of the potentials ϕ_j . This allows for an intuitive geometric understanding especially for planar graphs, which includes many important natural and man-made supply networks. In this case the fundamental cycles are simply given by the faces of the network, which form the so-called *dual graph* [8]. In particular, we obtain the following result for the cycle flows using only the topology of a planar network.

Proposition 1. *A perturbation of the capacity K_{e_0} of a single edge e_0 in a supply network induces cycle flows f_c which are to leading order given by equation (7). If the network is planar, then the dual graph can be decomposed into at most two connected subgraphs ('domains') \mathcal{D}_+ and \mathcal{D}_- , with $f_c \geq 0 \forall c \in \mathcal{D}_+$ and $f_c \leq 0 \forall c \in \mathcal{D}_-$. The domain boundary, if it exists, includes the perturbed edge e_0 , i.e. the two cycles adjacent to e_0 belong to different domains.*

A proof is given in appendix B. The implications of the proposition are illustrated in figure 1 (c), showing the induced cycle flows when the dashed edge is damaged such that its transmission capacity decreases. The cycle flows are positive in one domain and negative in the other domain. If the perturbed edge lies on the boundary of a finite network, then there is only one domain and all cycle flows are oriented in the same direction.

With this result we can obtain a purely geometric prediction of how the flow of all edges in the network change after the perturbation. For this, we need some additional information about the magnitude of the cycle flows in addition to the direction. We consider the upper and lower bound for the cycle flows f_c at a given distance to the cycle c_1 with $\kappa q_{c_1} > 0$ and the cycles c_2 with $\kappa q_{c_2} < 0$, respectively:

$$\begin{aligned} u_d &= \max_{c, \text{dist}(c, c_1)=d} f_c \\ \ell_d &= \min_{c, \text{dist}(c, c_2)=d} f_c. \end{aligned} \quad (10)$$

Proposition 2. *The maximum (minimum) value of the cycle flows decreases (increases) monotonically with the distance d to the reference cycles c_1 and c_2 , respectively:*

$$\begin{aligned} u_d &\leq u_{d-1}, & 1 \leq d \leq d_{\max}. \\ \ell_d &\geq \ell_{d-1}, & 1 \leq d \leq d_{\max}. \end{aligned} \quad (11)$$

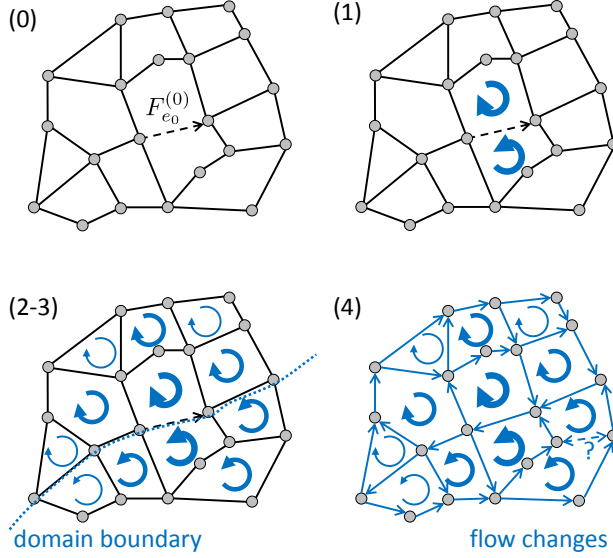


FIG. 1. Schematic representation of the algorithm 1 to predict flow changes after the damage ($\kappa < 0$) of a single edge (dashed).

We note that d denotes the distance of two cycles or faces, i.e. the length of the shortest path between the two faces in the dual graph. A proof is given in appendix C. Strict monotonicity can be proven when some additional technical assumptions are satisfied, which is expected to hold in most cases. In fact, one finds that the decay is rather fast for many networks of interest:

(1) For two-dimensional lattices with regular topology and edge weights the cycle flows decay with the inverse distance. A proof for square lattices in the continuum limit is given in appendix D.

(2) For two-dimensional lattices with regular topology but disordered edge weights, the eigenstates of A generally decay exponentially with the euclidean distance. This statement is a manifestation of Anderson localization and was confirmed numerically for many random network ensembles [9–12]. [13].

These results imply that the cycle flows $|f_c|$ decay rather rapidly with the distance such that the response of a supply network is confined to the ‘vicinity’ of the damaged edge. However, it has to be noted that the distance is defined for the dual graph, not the original graph, and that the rigorous results hold only for planar graphs. The situation is much more involved in non-planar graphs, as an edge can link regions which would be far apart otherwise.

We are thus in the position to predict the change of network flows after the perturbation of a single edge on a purely topological basis according to the following algorithm whose steps are illustrated in figure 1.

Algorithm 1. (*Prediction of flow changes*)

1. Assign a cycle flow to the cycles directly adjacent to the perturbed edge e_0 , denoted by c_1 and c_2 in the following. If $\kappa < 0$, these cycle flows are anti-

parallel to $F_{e_0}^{(0)}$, if $\kappa > 0$ the cycle flows are parallel to $F_{e_0}^{(0)}$.

2. Assign a cycle flow with the same orientation to all cycles adjacent to c_1 and c_2 . If a cycle is adjacent to both c_1 and c_2 , the flow direction for this cycle cannot be decided. Assume that the strength of the cycle flow is weaker.
3. Repeat this for the next-to-nearest neighbors and so on.
4. The direction of flow change of each edge is then given by the direction of the strongest cycle flow in the two adjacent cycles. The flow over a bridge and the flows in disconnected cycles remain unchanged.

IV. LINEAR FLOW IN PLANAR GRAPHS

In many important applications the flow is directly proportional to the potential drop along an edge of the network. Then the equation for the cycle flows (7) becomes exact, with $g \equiv 1$ and the matrix A given by

$$A_{d,c} = \sum_{e=1}^L C_{d,e} C_{c,e} \quad (12)$$

$$= \begin{cases} \text{No. of edges shared by faces } c \text{ and } d & \text{if } c \neq d \\ \text{No. of edges in face } c & \text{if } c = d. \end{cases}$$

Hence, the matrix A can be seen as a part of the Laplacian of the dual of G , the original network, excluding the row and column corresponding to the unbounded face of G . A formal solution of Eq. (7) shows that the induced cycle flow f_c depends on the topology of the network only via the so-called ‘resistance distances’ R to the cycles c_1 and c_2 ,

$$f_c \propto R_{c,c_1} - R_{c,c_2} \quad (13)$$

(for derivation see Appendix E). Resistance distances have been first introduced for networks of electric resistors, where they describe the effective resistance between two nodes [14], and provide a metric on graphs. XXX @ Debsanka: That’t nice, but what is it good for? XXX

Now we discuss how the decay of cycle flow differs in different network topologies.

To analyze how the topology affects the response of a flow network, in particular its decay with the distance, we simulate the flow change for a collection of regular and random lattices. For a square lattice, we find that the cycle flows are related to the distance from the source of the perturbation by a power law. Near the boundary of the finite network, decay becomes much more rapid (Figure 2). Topological randomness is introduced by merging a nodes with a randomly chosen neighbours with a small probability p . As we see in figure 2, the introduction of randomness slows down the decay of cycle flows. However, there still exists a region extending from the source

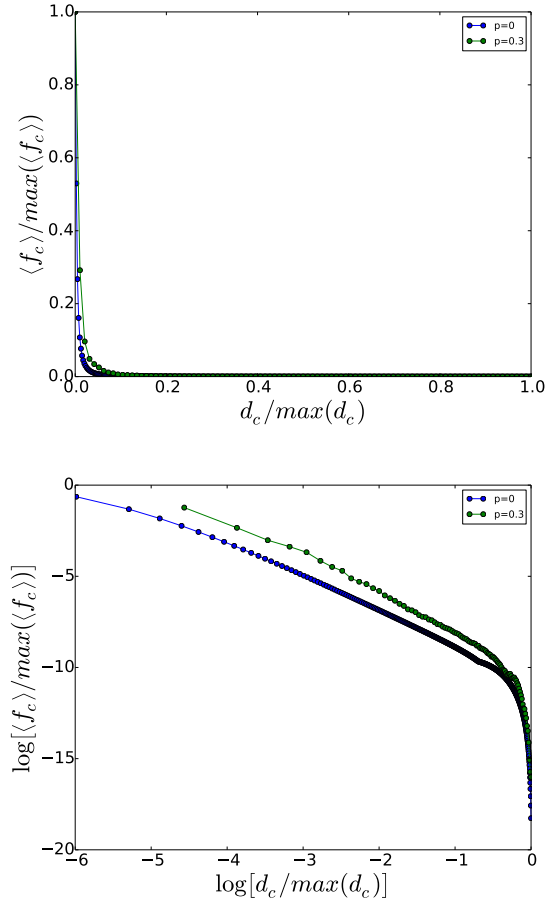


FIG. 2. (a) Decay of induced cycle flows in a square lattice of size 200x200 after the failure of the edge edge between nodes (0,0) and (0,1). (b) The log-log plot of the same showing power law decay

of the perturbation till 40% of the diameter of the graph where the decay of cycle flow is linear.

XXX Left: Flow strength in color code for a map of the lattice as in the paper by Kettemann et al. Right: Magnitude $|f_c|$ versus distance without, with small and with strong randomness. Make a statement if the numerical findings are consistent with the analytic results in appendix D. And please see my notes about the the appropriate length scale below...

Dear Henrik and Debsankha, I have two comments on your results. (1) In a previous version I recommended to show that the induced cycle flows are proportional to the initial flow of the failing edge. You have argued that this is trivial since the entire system is linear anyway. But this assumption is only partially true. If you vary the strength of the perturbation κ at a fixed edge then the response is trivially proportional to κ . And also if you vary $F_e^{(0)}$ for a fixed edge the response will be trivially proportional to $F_e^{(0)}$. That's what the equations (7) and (8) tell us, assuming that the system is linear such

that the function f is the identity such that the function g uis constant. However, I claim something which is much stronger. My numerical test with the power grids show that the reponse is proportional to $F_e^{(0)}$ regardless of which edge fails. The only thing that matters is the cycle distance between failing edge and the observed edge, where you measure the perturbation. For a cycle distance $d_c = 0$ the proportionality factor is one and the correlation is almost perfect. That is what I show in figure 6. It't not so easily to clearly explain the difference and to show its importance. But I do thing that it is very important since it shows the *universality* of our concept. All the topology is not so interesting after all. In the moment I think that we should illustrate this result in the section on random networks, but I am not sure.

(2) The second important question is what I tried to make clear on the telephone: What is the important length scale in a flow network. I argue that it is not the usual edge distance of two edges but the *cycle distance* of two edges. I give a rigorous definition below. Basically $d_c(e_0, e_1) = 0$ means that the two edges e_0 and e_1 are on the same cycle. I claim that all edges e_1 with $d_c(e_0, e_1) = 0$ are equally affected when the edge e_0 fails, regardless of their edge distance! For the power grid example this claim definitely holds as shown by the perfect correlation coefficient in (see figure 6 c). Open questions are: Does this hold generally also for random networks? Does it hold also for larger edge distances? To answer these two question we should simulate random planar networks with cycles of very different size and analyze which distance metric (edge vs. cycle) better predicts the decay of the response. I can think of different options to do so, and maybe you find an even better option: (a) Do plots as in figure 6, once with the cycle distance and once with the edge distance. I assume that the correlation factor R is much higher for the cycle distance. (b) Directly plot the normalized reponse $\Delta F_e / F_e^{(0)}$ as a function of the distance between e and e' and analyze the correlation by means of the correlation ratio or the mutual information, or I don't know. You have many experts on measuring correlations at MPI DS.

Definition of cycle distance: The strength of the cycle flows is expected to decay rapidly with the distance, which has to be understood as the graph-theoretic distance in the *dual* graph (called d_d in the following). Therefore also the change of the edge flows after a perturbation,

$$\Delta F_e = F'_e - F_e^{(0)} = \sum_{c=1}^{L-N+1} f_c C_{c,e}, \quad (14)$$

is expected to decay rapidly, where the relevant distance is still determined by the adjacent cycles. We thus define the cycle distance of two edges e_0 and e_1 as the minimum

distance of the adjacent cycles in the dual graph,

$$d_c(e_0, e_1) = \begin{cases} 0 & \text{if } |C_{c,e_0}| = |C_{c,e_1}| \forall c \\ \min_{\substack{c_0, c_1 \text{ s.t.} \\ |C_{c_0,e_0}|=1 \\ |C_{c_1,e_1}|=1}} d_d(c_0, c_1) + 1 & \text{otherwise.} \end{cases} \quad (15)$$

We note that this distance can be strongly different from the common edge distance (called d_e in the following), which is defined as the length of the shortest path from e_0 to e_1 in the respective line graph.

One remark. Maybe we should slightly change the definition by adding 1 to the formula 15 and defining $d_c(e, e) = 0$. Then we have a real distance in the mathematical sense. At least I hope so. We would still have to check the triangle inequality.

V. VASCULAR NETWORKS

Vascular plants possess an intricate, highly reticulate network supplying the leaf blade with water for gas exchange through evaporation as well as photosynthesis. The transport of water in these vascular networks can be described by a potential flow as shown in [2]. As leaf networks are naturally planar, our theorem can be used to predict the direction of flow changes after a damage to the leaf.

We demonstrate this by simulating the cycle flow arising from perturbing the main vein of one leaf of Norway maple (*Acer platanoides*). The leaf was chemically cleared and stained to make the complete network visible, then scanned at high resolution (3200 dpi) and the vascular network extracted using a vectorization approach. The result is a complete representation of the network topology and geometry. XXX Reference? XXX

Flow through an edge is described by $F_e = k \frac{R_e^4}{L_e} (p_{e_0} - p_{e_1})$, where R_e is edge radius, L_e is edge length, p_{e_i} is hydrostatic pressure at node e_i , and k is a constant of proportionality. This is basically Poiseuille's law.[15] The continuity equation is $\sum_e E_{i,e} F_e = P(1 + (N - 2)\delta_{i,0})$, modeling uniform evaporation of water over the whole leaf blade except at the petiole ($i = 0$), which acts as an inlet. XXX Can we use ϕ for the pressure as before and r for the radius? We already have capital R for the resistance distance. XXX

Since the flow equation is linear in the pressure difference, the flow change due to the perturbation is indeed exactly (up to a constant factor) described by equation (7). The simulation results are shown in figure 3. It is interesting to note that (a) the domain boundary between cycle flows of opposite orientation follows the leaf symmetry axis (the main vein) almost exactly. When perturbing other veins, the domain boundary similarly appears to follow the locally thickest veins. XXX Cool. Can we have a few more pictures of different leaves demonstrating this result for the appendix? XXX Additionally,

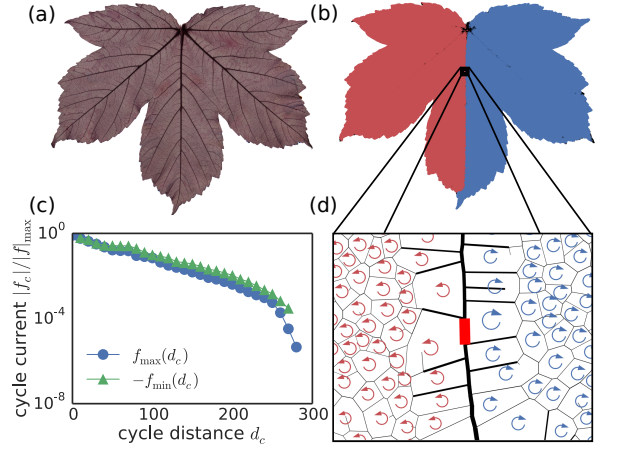


FIG. 3. (a) A leaf blade of Norway maple (*Acer platanoides*), high resolution scan (3200 dpi). The complete venation network up to all orders was extracted from this image. (b) The flow network as extracted from the high resolution scan. One edge on the main vein has been perturbed (approximate position shown by black rectangle), oppositely oriented cycle flows are marked in red and blue. The domain boundary clearly follows the main vein almost perfectly. (c) A semi-logarithmic plot of the absolute value of maximum (blue circles) and minimum (green triangles) cycle flow strength as a function of shortest path distance on the dual graph d_c from the perturbation. Formally, $f_{\max}(d_c) = \max_{d(c', c_{e_0})=d_c} f_{c'}$, where c_{e_0} is one of the cycles adjacent to the perturbed edge e_0 and $d(c, c')$ is the shortest path distance between cycles c and c' in the dual network. The definition of f_{\min} is similar. XXX Can we please use the same definition as in the text, in particular proposition 2 and just refer to it? XXX Solid lines act as a guide for the eye. Decay is approximately exponential, showing strong localization of the perturbation, compatible with results from Anderson localization. (d) Zoom to the region close to the perturbation. The perturbed edge is marked in bright red, oppositely oriented cycle currents are represented by oriented arrows. Arrow size is proportional to cycle flow magnitude, edge diameters are proportional to measured vein diameters but have been downsampled to improve clarity of the image. XXX Can we have one sentence in the beginning summarizing the main message of the figure and can we make the entire caption a bit shorter and more to the point? XXX

(b) cycle flow strength on either sides of thick veins appears to jump when there is no domain boundary, effectively confining the perturbation to a localized region. A different localization behavior (c) can be observed by plotting maximum and minimum cycle flow as a function of shortest path distance on the dual graph. XXX That's what I call cycle distance. We should have a consistent notation. And we should put the definition into the main text instead of the figure caption ;-) XXX Approximately exponential decay is clearly discernible over large distances. The leaf network is thus disordered enough to show Anderson localization of the perturbation. We speculate that this may be functionally relevant for the plant, as damage in one part of the leaf has only local ef-

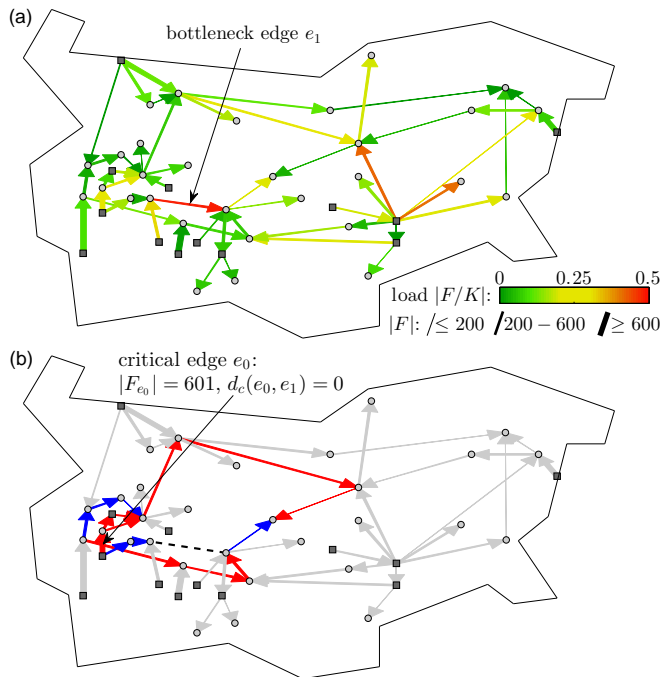


FIG. 4. Identification of critical transmission lines. (a) Model of the Bulgarian power transmission grid under extreme load (see text for details). Shown is direction and magnitude of the absolute power flow $|F|$ in MW as well as the relative load $|F/K|$ in a color code. One bottleneck edge e_1 in central Bulgaria is vulnerable to secondary overloads. (b) Algorithm 1 readily predicts which outage will lead to an increase (red) or decrease (blue) of the flow on the bottleneck edge e_1 . Only edges with a small cycle distance $d_c \leq 1$ are considered, as remote edges are expected to have no significant influence. In this way, one critical edge e_0 is identified which has a small distance $d_c(e_0, e_1) = 0$ and a high initial flow $|F_{e_0}| = 601$ MW.

fects, leaving most of the rest functioning undisturbedly.
XXX Cool Cool Cool. XXX

VI. PREDICTING BLACKOUTS IN POWER GRIDS

Power grids form the backbone of our technical infrastructure. Their stable operation is essential for our economy and everyday life [16, 17]. Generally, power grids must be operated such that they are resilient against the damage of a single transmission line (the so-called $n-1$ criterion [18]). Still, local failures repeatedly induce global outages in periods of extreme loads [17], which are expected to become much more likely in the future [19]. Any fundamental result that predicts the effects of local failures is thus of great scientific as well as economic value.

If ohmic losses can be neglected and the voltage magnitude U is constant throughout the grid, then the real

power flow between two nodes j and ℓ reads [20, 21]

$$F_{j,\ell} = U^2 B_{j\ell} \sin(\phi_j - \phi_\ell), \quad (16)$$

where ϕ_j is the power angle, i.e. the phase angle of the complex voltage at node j , and $B_{j\ell}$ is the admittance of the respective transmission line. The continuity equation for the real power is given by (1) such that our results can be used to analyze the consequences of transmission line failures. The case of non-vanishing losses is further analyzed in appendix A.

The topological response theory allows a direct assessment of transmission lines which are critical for network operation in the sense that their failure might induce a cascade leading to a network-wide outage. As an example, we analyze the operation of the Bulgarian power grid in a hypothetical situation of extreme load shown in figure 4 (a). The network model is based on the dataset [22], neglecting power im- and exports and increasing the generation and load at all nodes by a constant factor 50 % in comparison to the normal operation. The grid is no longer $n-1$ -secure in this situation. Can we predict which transmission line failures can induce secondary outages and thus a potentially catastrophic cascade of failures?

To find the Achilles' heel of the grid, we face the *inverse* problem as before. The starting point is the observation of one heavily loaded transmission line e_1 in central Bulgaria, which is vulnerable to secondary overloads (see figure 4 (a)). Then we have to calculate which perturbations in the grid would create the strongest response at the transmission line e_1 . First, applying algorithm 1 to all possible trigger edges e in the network reveals whether the load of e_1 increases or decreases when e fails. It increases when the flow change ΔF_{e_1} is parallel to the initial flow $F_{e_1}^{(0)}$, and decreases otherwise. Second, we have shown that the strength of the flow change are essentially determined by the initial flow of the failing edge and the cycle distance. In the current example we thus identify a single transmission lines with a cycle distance $d_c(e_0, e_1) = 0$ and a high initial flow $|F_{e_0}^{(0)}| = 601$ whose failure is predicted to increase the load at e_1 (see figure 4 (b)). Indeed, numerical simulations confirm that exactly this edges e_0 is indispensable for network operation. If it fails, no solution of the continuity equation can be found, which signals an impending blackout of the grid.

Notably, we also find several edges, whose removal would *reduce* the load of the vulnerable edge e_1 . Hence, the removal of a transmission line can be beneficial as it decreases the maximum load in the grid. This surprising behaviour has been first discussed by Braess for traffic networks in a game theoretic framework [23] and has recently been generalized to other types of supply network [24–26]. The topological response theory provides an intuitive explanation of this behaviour and shows that it is rooted in the cyclic topology of the network. In fact, it should occur for all types of network that respect the continuity equation.

VII. DISCUSSION

XXX TODO XXX

ACKNOWLEDGMENTS

We gratefully acknowledge support from the Helmholtz Association (grant no. VH-NG-1025) and the Federal Ministry of Education and Research (BMBF grant no. 03SF0472B and 03SF0472E).

Appendix A: Reponse theory for AC Power Grids

The state of an AC electric power grid is generally described by the so-called load flow equations for the real and the reactive power. They include ohmic losses such that the continuity equation (1) does not apply directly. However, the losses are generally small such that topological response theory can still provide a very good prediction of the state of the grid after a transmission line failure. In this appendix we briefly introduce the load flow equations and analyze the performance of this prediction for a common model power grid.

Consider grid with N_g generator nodes and N_l load nodes. The continuity equation for the real power reads [20]

$$P_k = \sum_{m=1}^{N_g+N_l} U_k U_m (G_{km} \cos \phi_{km} + B_{km} \sin \phi_{km}), \quad (\text{A1})$$

where P_k is the power generation or demand at node k , $U_k e^{i\phi_k}$ is the complex voltage and $\phi_{km} = \phi_k - \phi_m$ abbreviates the phase difference. The coupling of the nodes is described by the nodal admittance matrix $Y_{km} = G_{km} + iB_{km}$. If all voltages are constant, $U_k = U$ and ohmic losses can be neglected ($G_{km} = 0$), then we recover the continuity equation in the form discussed in section II,

$$P_k = \sum_{m=1}^{N_g+N_l} U^2 B_{km} \sin(\phi_k - \phi_m). \quad (\text{A2})$$

These approximations are mostly satisfied in modern power grids. Even more, a linearization as in equation (7) is appropriate when the grid is not too heavily loaded, which yields the so-called DC approximation [20, 27]. Most power grids are approximately planar, crossings of transmission lines are possible but rare. We thus expect that the algorithm 1 can still predict the effects of the damage of single transmission lines in real power grids with great accuracy.

We test the algorithm for the 30 bus test grid from [28] using both the full AC load flow calculations including ohmic losses and the DC approximation. In the AC case, the voltage U_k of the consumer nodes are free variables

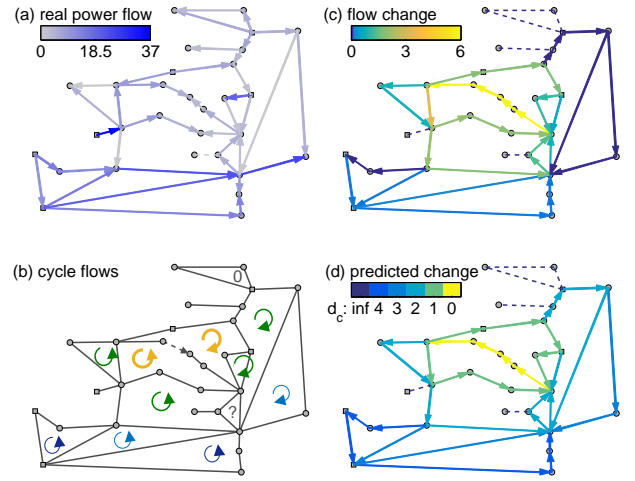


FIG. 5. Predicting flow changes after a transmission line failure in a model power grid. (a) Real power flows in the initial intact network in MW. (b) The failure of a transmission line (dashed) must be compensated by cycle flows indicated by cyclic arrows. The thickness of the lines indicates the strength of the cycle flows. (c) The resulting flow changes after the failure of the marked transmission line. (d) The direction of the flow changes are exactly predicted by algorithm 1 for all edges and the magnitude decreases with the cycle distance d_c . The power flow in (a,c) has been calculated using the standard software MATPOWER for the 30-bus test case [28]. The cycle flows and the flow changes in (b,d) have been determined by algorithm 1.

whereas the reactive power demand is fixed which yields the additional constraint [20]

$$Q_k = \sum_{\ell=1}^{N_g+N_l} U_k U_m (G_{km} \sin \phi_{km} - B_{km} \cos \phi_{km}). \quad (\text{A3})$$

In total, we have $2N_g + N_l$ free variables (N_l voltages and $N_g + N_l$ phase angles) to satisfy the $2N_g + N_l$ nonlinear equations (A1) and (A3). Figure 5 compares numerically exact values for the real power flows and the flow changes after the failure of a single transmission line with the topological predictions using algorithm 1. The direction of the flow changes is correctly predicted for all edges. Notably, the flow changes are zero for one disconnected cycle in the north and several bridges. The strength of the flow changes depends primarily on the cycle distance to the failing edge, as shown in panels (c) and (d).

To reveal the essential factors which determine the response of a power grid to a local failure, We perform a full $n - 1$ -simulation of the 30 bus test grid, i.e. we sample over all possible trigger edges and calculate the flow change for all remaining edges. Figure 6 (a) shows that the flow change at the remaining edges depends linearly on the flow of the failing edge F_{e_0} . For a cycle distance $d_c = 0$ we observe an almost perfect proportionality while for larger distances other factors become more and more important. Still, we find a strong linear correlation also for larger distances, see panel (c). The normalized flow

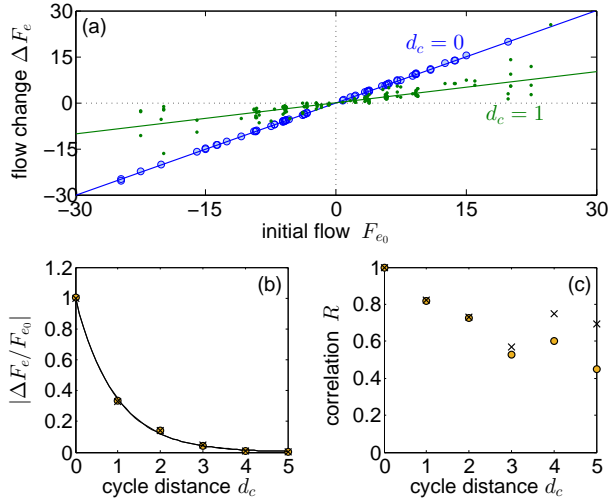


FIG. 6. The reponse of a power grid to a transmission line failure increases linearly with the flow of the failing line and decay exponentially with the cycle distance. (a) Flow change ΔF_e as a function of the initial flow of the failing line F_{e_0} for all pairs of lines e and e_1 with cycle distance $d_c = 0$ (blue circles) and $d_c = 1$ (green dots). Solid lines are linear fits. (b) Decay of the flow change, normalized by the initial flow of the failing edge, with the cycle distance. Symbols are numerical values averaged over all edge pairs with a given cycle distance d_c . The black line shows an exponential fit. (c) Correlation coefficients for the linear relation in panel (a) as a function of the cycle distance. An almost perfect proportionality is found for $d_c = 0$. The power flow has been calculated using MATPOWER for the 30-bus test case [28] with the full load flow equations (circles) and within the DC approximation (crosses, only in panels b,c). Results have been collected for all pairs of failing edge e_0 and affected edge e .

change decays rapidly with the cycle distance as shown in panel (b). An exponential fit shows an excellent agreement.

In panels (b) and (c) we further compare the results of the full nonlinear load flow equation with the lossless, linear DC approximation. Although our theory applies rigorously only to the lossless model, we observe a very good agreement in both cases. We conclude that topological reponse theory yields good results also for power grids with moderate losses.

Appendix B: Proof of proposition 1

In the following we analyze the solution of equation (7). W.l.o.g. we assume that both the original network and the dual graph are connected. Otherwise we can just focus on the connected component which includes the perturbed edge resp. the perturbed cycles and exclude all disconnected parts from our analysis.

Definition 1. A positive domain \mathcal{D}_+ is a connected sub-graph of the dual with $f_c \geq 0$ for all $c \in \mathcal{D}_+$ and at least one cycle with $f_c > 0$. The domain \mathcal{D}_+ is called isolated

if $f_d \leq 0$ for all cycles d in the immediate neighborhood of the domain \mathcal{D}_+ . Analogously we use \mathcal{D}_- for a domain with opposite signs.

Definition 2. We denote by \mathcal{B} the set of edges which form the boundary of the graph, i.e. the set of edges which is adjacent to only one cycle in the dual graph:

$$\mathcal{B} = \left\{ e \in E \mid \sum_c C_{ce} \neq 0 \right\}. \quad (\text{B1})$$

Lemma 2. Each isolated domain \mathcal{D}_+ must contain a cycle c_1 with $q_{c_1} > 0$ and each isolated domain \mathcal{D}_- must contain a cycle c_2 with $q_{c_2} < 0$.

Proof. To proof this statement assume the opposite: Let \mathcal{D}' be a domain with $f_c \geq 0$ and $\kappa q_c \leq 0$ for all $c \in \mathcal{D}'$ and at least one cycle with $f_c > 0$. Using equation (7) we find that

$$\begin{aligned} \sum_{c \in \mathcal{D}'} A_{cc} f_c &= - \sum_{c \in \mathcal{D}'} \sum_{d \neq c} A_{cd} f_d + \sum_{c \in \mathcal{D}'} \kappa q_c \\ &= - \sum_{c \in \mathcal{D}'} \sum_{\substack{d \in \mathcal{D}' \\ d \neq c}} A_{cd} f_d - \sum_{c \in \mathcal{D}'} \sum_{d \notin \mathcal{D}'} A_{cd} f_d \\ &\quad + \sum_{c \in \mathcal{D}'} \kappa q_c. \end{aligned} \quad (\text{B2})$$

Furthermore, using the definition (8) of the matrix A , we have

$$A_{cc} = - \sum_{d \neq c} A_{dc} + \sum_{e \in \mathcal{B}} C_{ce}^2 g_e \quad (\text{B3})$$

such that

$$\begin{aligned} \sum_{c \in \mathcal{D}'} A_{cc} f_c &= - \sum_{c \in \mathcal{D}'} \sum_{\substack{d \in \mathcal{D}' \\ d \neq c}} A_{cd} f_c - \sum_{c \in \mathcal{D}'} \sum_{d \notin \mathcal{D}'} A_{cd} f_c \\ &\quad + \sum_{c \in \mathcal{D}'} \sum_{e \in \mathcal{B}} C_{ce}^2 g(F_e^{(0)}/K_e). \end{aligned} \quad (\text{B4})$$

Comparing the two expressions and using the symmetry $A_{cd} = A_{dc}$ we find that

$$\begin{aligned} &- \sum_{c \in \mathcal{D}'} \sum_{d \notin \mathcal{D}'} A_{cd} f_d + \sum_{c \in \mathcal{D}'} \kappa q_c \\ &= - \sum_{c \in \mathcal{D}'} \sum_{d \notin \mathcal{D}'} A_{dc} f_c + \sum_{c \in \mathcal{D}'} \sum_{e \in \mathcal{B}} C_{ce}^2 g(F_e^{(0)}/K_e). \end{aligned} \quad (\text{B5})$$

This leads to a contradiction as the left-hand side of the equation is smaller or equal to zero, while the right-hand side is larger than zero. Hence, the assumption must be wrong and no such domain \mathcal{D}' exists. \square

Corrolary 1. Consider the solution of equation (7) if exactly one edge e_0 is perturbed or damaged.

If the edge e_0 lies in the interior of the graph ($e_0 \notin \mathcal{B}$), then we have $\kappa q_{c_1} > 0$ and $\kappa q_{c_2} = -\kappa q_{c_1} < 0$ for the two cycles c_1, c_2 adjacent to the edge e_0 and $q_c = 0$ otherwise.

Then \mathcal{D}_+ contains the cycle c_1 and \mathcal{D}_- contains the cycle c_2 and no further isolated domains can exist.

If the edge e_0 lies on the boundary of the graph ($e_0 \in \mathcal{B}$), then only a single cycle c_1 is affected with $q_{c_1} \neq 0$. Hence there is only one domain in the graph such that $f_c \geq 0$ for all cycles c if $q_{c_1} > 0$ and $f_c \leq 0$ for all cycles c if $q_{c_1} < 0$.

Appendix C: Proof of proposition 2

As before we analyze the solution of equation (7) and assume that both the original network and the dual graph are connected. In the following we denote by $\text{dist}(c, c')$ the graph theoretic distance of two vertices c and c' of the dual graph.

Definition 3. We denote by u_d (ℓ_d) the maximum (minimum) value of cycle flows f_c for all vertices c of the dual graph with a given distance d to a reference vertex c' :

$$\begin{aligned} u_d &= \max_{c, \text{dist}(c, c')=d} f_c \\ \ell_d &= \min_{c, \text{dist}(c, c')=d} f_c. \end{aligned} \quad (\text{C1})$$

Lemma 3. The maximum value of the cycle flows u_d decreases monotonically with the distance to the reference cycle c_1 for which $\kappa_{c_1} > 0$:

$$u_d \leq u_{d-1}, \quad 1 \leq d \leq d_{\max}. \quad (\text{C2})$$

The minimum ℓ_d increases monotonically with the distance to the reference cycle c_2 for which $\kappa_{c_2} < 0$:

$$\ell_d \geq \ell_{d-1}, \quad 1 \leq d \leq d_{\max}. \quad (\text{C3})$$

Proof. The proof is carried out by induction starting from $d = d_{\max}$. We only give the proof for the maximum, the proof for the minimum proceeds in an analog way.

(1) Base case $d = d_{\max}$: Consider the vertex c of the dual for which $\text{dist}(c, c_1) = d_{\max}$ and f_c assumes its maximum $f_c = u_{d_{\max}}$. Equation (7) yields

$$\begin{aligned} A_{cc}f_c &= - \sum_{b \neq c} A_{cb}f_b \\ &= - \sum_{\substack{b \neq c \\ \text{dist}(b, c_1)=d_{\max}}} A_{cb}f_b + \sum_{\substack{b \neq c \\ \text{dist}(b, c_1)=d_{\max}-1}} A_{cb}f_b. \end{aligned} \quad (\text{C4})$$

We define the abbreviations

$$\mathcal{A}_d = - \sum_{b \neq c, \text{dist}(b, c_1)=d} A_{cb} \quad (\text{C5})$$

and use some important properties of the matrix A :

$$\begin{aligned} A_{cb} \leq 0 \text{ for } c \neq b &\Rightarrow \mathcal{A}_d \geq 0 \\ A_{cc} \geq \mathcal{A}_{d_{\max}} + \mathcal{A}_{d_{\max}-1}. & \end{aligned} \quad (\text{C6})$$

We can furthermore bound the values of f_b in equation (C4) by $u_{d_{\max}}$ or $u_{d_{\max}-1}$, respectively, such that we obtain

$$\begin{aligned} u_{d_{\max}} = f_c &\leq \frac{\mathcal{A}_{d_{\max}}u_{d_{\max}} + \mathcal{A}_{d_{\max}-1}u_{d_{\max}-1}}{\mathcal{A}_{d_{\max}} + \mathcal{A}_{d_{\max}-1}} \\ \Rightarrow u_{d_{\max}} &\leq u_{d_{\max}-1}, \end{aligned} \quad (\text{C7})$$

(2) Inductive step $d \rightarrow d-1$: We consider the vertex c with $\text{dist}(c, c_1) = d$ and $f_c = u_d$. Starting from equation (7) and using the same estimations as above, we obtain

$$\begin{aligned} u_d = f_c &= \frac{\kappa q_c - \sum_b A_{cb}f_b}{A_{cc}} \\ &\leq \frac{\mathcal{A}_{d-1}u_{d-1} + \mathcal{A}_d u_d + \mathcal{A}_{d+1}u_{d+1}}{\mathcal{A}_{d-1} + \mathcal{A}_d + \mathcal{A}_{d+1}}. \end{aligned} \quad (\text{C8})$$

Note that the inhomogeneity $\kappa q_c \leq 0$ for all vertices except for $c = c_1$. With the induction hypothesis $u_{d+1} \leq u_d$ this yields

$$\begin{aligned} u_d &\leq \frac{\mathcal{A}_{d-1}u_{d-1} + (\mathcal{A}_d + \mathcal{A}_{d+1})u_d}{\mathcal{A}_{d-1} + \mathcal{A}_d + \mathcal{A}_{d+1}} \\ \Rightarrow u_d &\leq u_{d-1}. \end{aligned} \quad (\text{C9})$$

which completes the proof. \square

Lemma 4. The maximum (minimum) value of the cycle flows u_d decreases (increases) strictly monotonically with the distance to the reference cycle c_1 (c_2)

$$\begin{aligned} u_d &< u_{d-1}, \\ \ell_d &> \ell_{d-1}, \quad 1 \leq d \leq d_{\max}. \end{aligned} \quad (\text{C10})$$

if (1) all cycles c at maximum distance from c_1 lie at the boundary of the dual graph,

$$\forall c \text{ with } \text{dist}(c, c_1) = d_{\max} : \quad (\text{C11})$$

$$\exists \text{ edge } e \text{ with } e \in \mathcal{B} \text{ and } C_{ce} \neq 0. \quad (\text{C12})$$

or (2) all extrema u_d and ℓ_d are unique.

Proof. We show that in both cases we can replace \geq by $>$ in the base case and thus also in the inductive step in the proof of lemma 3. If condition (1) is satisfied we have

$$A_{cc} > \mathcal{A}_{d_{\max}} + \mathcal{A}_{d_{\max}-1} \quad (\text{C13})$$

due to boundary terms. If condition (1) is not satisfied but condition (2) is, then the sum in equation C4 includes at least two terms. One of the values of f_b in the sum must be strictly smaller than the maximum value u_d or u_{d-1} , respectively, as we assumed that these maxima are unique. We thus can replace the \geq by $<$ in the estimations. \square

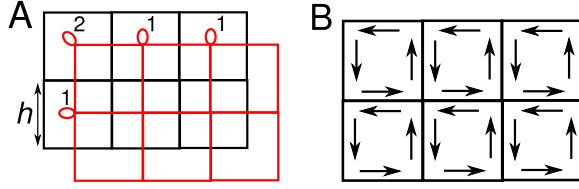


FIG. 7. A. A square lattice (black) together with its cycle dual (red). The cycle dual is also a square lattice, but because the boundary edges are only adjacent to one cycle, it contains self-loops at its boundary nodes. The weight of a self loop is the sum of all boundary edge weights which are part of the boundary cycle. In the limit $h \rightarrow 0$, the self-loops enforce Dirichlet boundary conditions on the cycle density, $\phi|_{\partial A} = 0$. B. Consistently oriented cycles in a square lattice.

Appendix D: Decay in regular lattices

In this appendix we derive the continuum model directly from the discrete network model in the uniform case. Consider a network with cycle edge adjacency matrix C_{ce} . Then we are interested in a continuous version of equation (7). On a square lattice the application of A_{cd} to a vector in the bulk can be written, going to the continuous limit (see Fig. 7),

$$(A\phi)(x) = \frac{\phi(x, y)}{K(x + h/2, y)} + \frac{\phi(x, y)}{K(x - h/2, y)} \quad (D1)$$

$$+ \frac{\phi(x, y)}{K(x, y + h/2)} + \frac{\phi(x, y)}{K(x, y - h/2)} \quad (D2)$$

$$- \frac{\phi(x + h, y)}{K(x + h/2, y)} - \frac{\phi(x - h, y)}{K(x - h/2, y)} \quad (D3)$$

$$- \frac{\phi(x, y + h)}{K(x, y + h/2)} - \frac{\phi(x, y - h)}{K(x, y - h/2)} \quad (D4)$$

$$= h^2 \nabla \cdot \left(\frac{1}{K} \nabla \phi \right) + O(h^3). \quad (D5)$$

Here, h is the lattice spacing. The right hand side works similarly, noting that only two cycles contribute, with opposite signs. Let us assume that e_0 is parallel to the y axis. Then the RHS is

$$- v_y(x + h/2, y) \frac{\kappa}{K(x + h/2, y)(K(x + h/2, y) - \kappa)} \quad (D6)$$

$$\times \delta^{(2)}(x + h/2, y) \quad (D7)$$

$$+ v_y(x - h/2, y) \frac{\kappa}{K(x - h/2, y)(K(x - h/2, y) - \kappa)} \quad (D8)$$

$$\times \delta^{(2)}(x - h/2, y) \quad (D9)$$

$$= h \frac{\partial}{\partial x} \left(v_y \frac{\kappa}{K(K - \kappa)} \delta^{(2)}(x, y) \right) + O(h^3). \quad (D10)$$

This is a dipole source field with dipole moment parallel to the x axis. It is easy to see the generalization

to arbitrary dipole moments. Thus, the full continuous equations governing the behaviour of the cycle density in the bulk are

$$\nabla \cdot \left(\frac{1}{K} \nabla \phi \right) = -\mathbf{p} \cdot \nabla \delta^{(2)}(\mathbf{x} - \mathbf{a}), \quad (D11)$$

for a perturbation at \mathbf{a} . The dipole vector \mathbf{p} is orthogonal in direction to flow at the site of perturbation and proportional in magnitude. More perturbations can be handled by linear combination. Note that we have subsumed the factors of h into the derivative by a change of variables $\mathbf{x} \rightarrow h\mathbf{x}$.

At the boundary, a similar relation as in the bulk holds, supplying us with boundary conditions. Because boundary cycles possess three neighboring cycles four edges in total, some terms are left over;

$$(A\phi)(x) = \frac{\phi(x, y)}{K(x + h/2, y)} + \frac{\phi(x, y)}{K(x - h/2, y)} \quad (D12)$$

$$+ \frac{\phi(x, y)}{K(x, y + h/2)} + \frac{\phi(x, y)}{K(x, y - h/2)} \quad (D13)$$

$$- \frac{\phi(x + h, y)}{K(x + h/2, y)} - \frac{\phi(x - h, y)}{K(x - h/2, y)} \quad (D14)$$

$$- \frac{\phi(x, y + h)}{K(x, y + h/2)} - \frac{\phi(x, y - h)}{K(x, y - h/2)} \quad (D15)$$

$$= \frac{\phi(x, y)}{K(x, y)} + O(h). \quad (D16)$$

Thus, we find that Dirichlet boundary conditions must hold in the absence of boundary perturbations: $\phi|_{\partial A} = 0$.

Finally, we need a law telling us how to calculate a flow vector from the cycle density. To this end, consider Figure 7 B. In order to obtain the y component of a flow vector, we need to add up the contributions of two cycle flows neighboring in the x direction, and vice versa. Thus, the flow vector becomes

$$\mathbf{v}(\mathbf{x}) = \begin{pmatrix} \phi(x, y + h/2) - \phi(x, y - h/2) \\ \phi(x - h/2, y) - \phi(x + h/2, y) \end{pmatrix} \quad (D17)$$

$$= \begin{pmatrix} 0 & 1 \\ -1 & 0 \end{pmatrix} \nabla \phi + O(h), \quad (D18)$$

where we again rescaled $\mathbf{x} \rightarrow h\mathbf{x}$.

In the case of uniform conductivity density $K(\mathbf{x}) \equiv K$, equation (D11) becomes a regular Poisson equation in two dimensions with dipole source density. The solutions to this equation are well known from the theory of electrostatics, on an infinite domain taking the form

$$\phi(\mathbf{x}) = \frac{\mathbf{p} \cdot \mathbf{x}}{x^2} \quad (D19)$$

$$\mathbf{v}(\mathbf{x}) = \begin{pmatrix} 0 & 1 \\ -1 & 0 \end{pmatrix} \left(\frac{\mathbf{p}}{x^2} - 2\mathbf{x} \frac{\mathbf{p} \cdot \mathbf{x}}{x^4} \right) \quad (D20)$$

for a perturbation at $\mathbf{a} = 0$. Indeed, the cycle density decays as $\phi(r) \sim r^{-1}$ and the flow due to the perturbation as $\mathbf{v}(r) \sim r^{-2}$.

Appendix E: Relationship between cycle flow and resistance distance

For linear flows, as discussed in IV, the equation (7) governing cycle flows

$$Af_c = \kappa q_d \quad (\text{E1})$$

is exact and equation (8) for the matrix A simplifies to

$$A_{d,c} = \sum_{e=1}^L C_{d,e} C_{c,e} \quad (\text{E2})$$

$$= \begin{cases} \text{No. of edges shared by faces } c \text{ and } d & \text{if } c \neq d \\ \text{No. of edges in face } c & \text{if } c = d. \end{cases}$$

Then the matrix A can be seen as a part of the Laplacian of the dual Graph (cf. [6, 29]) of G , the original network. Let L be a full Laplacian of the dual graph $D(G)$, whose 1st row corresponds to the *unbounded face* of G . Then A can be simply obtained by deleting the first row and first column of L .

$$L = \left(\begin{array}{c|ccc} L_{11} & L_{12} & L_{13} & \cdots \\ L_{21} & & & \\ L_{31} & & A & \\ L_{41} & & & \end{array} \right)$$

[6]

Now, equation (E1) is equivalent to the the auxiliary equation

$$Lf' = \kappa q'_d \quad (\text{E3})$$

$$f'[1] = 0 \quad (\text{E4})$$

where $q'_d = 0 \otimes q_d$. This equation can be formally solved as

$$f' = \kappa L^+ q'_d, \quad (\text{E5})$$

Where L^+ is the Moore-Penrose pseudoinverse of L . Now, the Moore-Penrose pseudoinverse is closely related to the resistance distance, which provides a metric on graphs [14]. In particular, the elements of L^+ are given by

$$L_{ij}^+ = -\frac{R_{ij}}{2} + \frac{1}{2|V|} (R_i^{\text{tot}} + R_j^{\text{tot}})$$

where R_{ij} is the resistance distance between the faces i and j and R_i^{tot} is the total resistance of all edges connected to node i . Plugging these relations into equation (E5), we obtain

$$f_c = \kappa (R_{c,c_0} - R_{c,c_1}) + \text{const}$$

-
- [1] M. Durand and D. Weaire, Phys. Rev. E **70**, 046125 (2004).
 - [2] E. Katifori, G. J. Szöllösi, and M. O. Magnasco, Phys. Rev. Lett. **104**, 048704 (2010).
 - [3] Y. Kuramoto, in *International Symposium on Mathematical Problems in Theoretical Physics*, edited by H. Araki (Springer, New York, 1975), Lecture Notes in Physics Vol. 39, p. 420.
 - [4] S. H. Strogatz, Physica D: Nonlinear Phenomena **143**, 1 (2000).
 - [5] J. A. Acebrón, L. L. Bonilla, C. J. Pérez Vicente, F. Ritort, and R. Spigler, Rev. Mod. Phys. **77**, 137 (2005).
 - [6] M. E. J. Newman, *Networks – An Introduction* (Oxford University Press, Oxford, 2010).
 - [7] D. Manik et al., Eur. Phys. J. Special Topics **223**, 2527 (2014).
 - [8] R. Diestel, *Graph Theory* (Springer, New York, 2010).
 - [9] B. Kramer, T. Ohtsuki, and S. Kettemann, Physics Reports **417**, 211 (2005).
 - [10] R. Huang, G. Korniss, and S. K. Nayak, Phys. Rev. E **80**, 045101 (2009).
 - [11] S. K. (Ed.), ed., *Localisation 2011* (World Scientific, Singapore, 2012).
 - [12] D. Labavic, R. Suci, H. Meyer-Ortmanns, and S. Kettemann, The European Physical Journal Special Topics **223**, 2517 (2014).
 - [13] Note1, in lattices with subgrid symmetry states exist which decay exponentially with the square root of the distance.
 - [14] D. Klein and M. Randić, Journal of Mathematical Chemistry **12**, 81 (1993).
 - [15] Note2, recent work has shown that in reality, there a scaling relationship between effective hydraulic diameter d_{eff} and external vein diameter R , $d_{\text{eff}} \sim R^{1-\gamma/4}$ with $\gamma \approx 0.6$. The radius parameter in Poiseuille's law should therefore really be corrected in this way. However, this relationship is not relevant for the point of this paper.
 - [16] S. H. Strogatz, Nature **410**, 268 (2001).
 - [17] P. Pourbeik, P. Kundur, and C. Taylor, IEEE Power and Energy Magazine **4**, 22 (2006).
 - [18] European Network of Transmission System Operators for Electricity, *Continental europe operation handbook*, <https://www.entsoe.eu/publications/system-operations-reports/operation-handbook> (retrieved 20/03/2015) (2004).
 - [19] T. Pesch, H.-J. Allelein, and J.-F. Hake, Eur. Phys. J. Special Topics **223**, 2561 (2014).
 - [20] A. J. Wood, B. F. Wollenberg, and G. B. Sheblé, *Power Generation, Operation and Control* (John Wiley & Sons, New York, 2013).
 - [21] M. Rohden, A. Sorge, M. Timme, and D. Witthaut, Phys. Rev. Lett. **109**, 064101 (2012).
 - [22] N. Hutcheon and J. Bialek, in *PowerTech (POWERTECH), 2013 IEEE Grenoble* (2013).
 - [23] D. Braess, Unternehmensforschung **12**, 258 (1968).
 - [24] A. E. Motter, Phys. Rev. Lett. **93**, 098701 (2004).
 - [25] D. Witthaut and M. Timme, New J. Phys. **14**, 083036 (2012).

- [26] D. Witthaut and M. Timme, Eur. Phys. J. B **86**, 377 (2013).
- [27] D. Van Hertem, J. Verboomen, K. Purchala, R. Belmans, and W. Kling, in *The 8th IEEE International Conference on AC and DC Power Transmission* (2006), pp. 58–62.
- [28] R. D. Zimmerman, C. E. Murillo-Sanchez, and R. J. Thomas, IEEE Transactions on Power Systems **26**, 12 (2011).
- [29] F. Levstein, C. Maldonado, and D. Penazzi, arXiv preprint arXiv:0906.0116 (2009).